

---

# Mean-Variance Policy Iteration for Risk-Averse Reinforcement Learning

---

**Shangtong Zhang** <sup>\*</sup>  
University of Oxford

**Bo Liu**  
Auburn University

**Shimon Whiteson**  
University of Oxford

## Abstract

We present a mean-variance policy iteration (MVPI) framework for risk-averse control in a discounted infinite horizon MDP. MVPI enjoys great flexibility in that *any policy evaluation method and risk-neutral control method can be dropped in for risk-averse control off the shelf, in both on- and off-policy settings*. We propose risk-averse TD3 as an example instantiating MVPI, which outperforms vanilla TD3 and many previous risk-averse control methods in challenging Mujoco robot simulation tasks under a risk-aware performance metric. This risk-averse TD3 is the first to introduce deterministic policies and off-policy learning into risk-averse reinforcement learning, both of which are key to the performance boost we show in Mujoco domains. MVPI adopts a per-step reward perspective (Bisi et al., 2019) for risk-averse control, instead of the commonly used total reward perspective.

## 1 Introduction

One fundamental task in reinforcement learning (RL, Sutton and Barto 2018) is control, in which we seek a policy that maximizes certain performance metrics. In risk-neutral RL, the performance metric is usually the expectation of some random variable, for example, the expected total (discounted or undiscounted) reward (Puterman, 2014; Sutton and Barto, 2018). We, however, sometimes want to minimize certain risk measures of that random variable while maximizing its expectation. For example, a portfolio manager usually wants to reduce the risk of a portfolio while maximizing its return. Risk-averse RL is a framework for studying such problems.

Although many real-world applications can potentially benefit from risk-averse RL, e.g., pricing (Wang, 2000), healthcare (Parker, 2009), portfolio management (Lai et al., 2011), autonomous driving (Matthaei et al., 2015), and robotics (Majumdar and Pavone, 2020), the development of risk-averse RL largely falls behind risk-neutral RL. Risk-neutral RL methods have enjoyed superhuman performance in many domains, e.g., Go (Silver et al., 2016), protein design (Senior et al., 2018), DoTA (OpenAI, 2018), and StarCraft II (Vinyals et al., 2019), while no human-level performance has been reported for risk-averse RL methods in real-world applications. Risk-neutral RL methods have enjoyed stable off-policy learning (Watkins and Dayan, 1992; Maei, 2011; Fujimoto et al., 2018; Haarnoja et al., 2018), while state-of-the-art risk-averse RL methods, e.g., Xie et al. (2018); Bisi et al. (2019), still require on-policy samples. Risk-neutral RL methods have exploited deep neural network function approximators and distributed training (Mnih et al., 2016; Espeholt et al., 2018), while tabular and linear methods still dominate the experiments of risk-averse RL literature (Tamar et al., 2012; Prashanth and Ghavamzadeh, 2013; Xie et al., 2018; Chow et al., 2018). Such a big gap between risk-averse RL and risk-neutral RL gives rise to a natural question: *can we easily make use of the recent advances in risk-neutral RL for risk-averse RL?* In this paper, we give an affirmative answer via the mean-variance policy iteration (MVPI) framework.

---

<sup>\*</sup>Correspondence to shangtong.zhang@cs.ox.ac.uk

Although many risk measures have been used in risk-averse RL, in this paper, we mainly focus on variance (Sobel, 1982; Mannor and Tsitsiklis, 2011; Tamar et al., 2012; Prashanth and Ghavamzadeh, 2013; Xie et al., 2018) given its advantages in interpretability and computation (Markowitz and Todd, 2000; Li and Ng, 2000). Such an RL paradigm is usually referred to as mean-variance RL, and previous mean-variance RL methods usually consider the variance of the total reward random variable (Tamar et al., 2012; Prashanth and Ghavamzadeh, 2013; Xie et al., 2018). Recently, Bisi et al. (2019) propose a reward-volatility risk measure. The reward-volatility considers the variance of a per-step reward random variable, which bounds the variance of the total reward from above, indicating that minimizing the variance of the per-step reward implicitly minimizes the variance of the total reward. Bisi et al. (2019) also show that the variance of the per-step reward can better capture the short-term risk than the variance of the total reward.

In this paper, we further argue that the variance of the per-step reward is easier to optimize than the variance of the total reward, and therefore develop MVPI under the per-step reward perspective. MVPI enjoys great flexibility in that *any policy evaluation method and risk-neutral control method can be dropped in for risk-averse control off the shelf, in both on- and off-policy settings*. Key to the flexibility of MVPI is the introduction of the Fenchel duality and cyclic coordinate maximization, which address the triple-sampling issue and the policy-dependent-reward issue in Bisi et al. (2019). Here the triple-sampling issue refers to a requirement of three independent sets of samples, and the policy-dependent-reward issue refers to a requirement to solve an MDP whose reward function depends on the policy being followed. We propose risk-averse TD3 (Fujimoto et al., 2018) as an example instantiating MVPI, which outperforms vanilla TD3 and many previous mean-variance RL methods (Tamar et al., 2012; Prashanth and Ghavamzadeh, 2013; Xie et al., 2018; Bisi et al., 2019) in challenging Mujoco robot simulation tasks in terms of a risk-averse performance metric. To the best of our knowledge, we are the first to benchmark mean-variance RL methods in Mujoco domains, a widely used benchmark for robotic-oriented RL research, and the first to bring off-policy learning and deterministic policies into mean-variance RL.

## 2 Mean-Variance RL

We consider an infinite horizon MDP with a state space  $\mathcal{S}$ , an action space  $\mathcal{A}$ , a bounded reward function  $r : \mathcal{S} \times \mathcal{A} \rightarrow \mathbb{R}$ , a transition kernel  $p : \mathcal{S} \times \mathcal{S} \times \mathcal{A} \rightarrow [0, 1]$ , an initial distribution  $\mu_0 : \mathcal{S} \rightarrow [0, 1]$ , and a discount factor  $\gamma \in [0, 1]$ . The initial state  $S_0$  is sampled from  $\mu_0$ . At time step  $t$ , an agent takes an action  $A_t$  according to  $\pi(\cdot | S_t)$ , where  $\pi : \mathcal{A} \times \mathcal{S} \rightarrow [0, 1]$  is the policy followed by the agent. The agent then gets a reward  $R_{t+1} \doteq r(S_t, A_t)$  and proceeds to the next state  $S_{t+1}$  according to  $p(\cdot | S_t, A_t)$ . In this paper, we consider a deterministic reward setting for the ease of presentation, following Chow (2017); Xie et al. (2018). The return at time step  $t$  is defined as  $G_t \doteq \sum_{i=0}^{\infty} \gamma^i r(S_{t+i}, A_{t+i})$ . When  $\gamma < 1$ ,  $G_t$  is always well defined. When  $\gamma = 1$ , to ensure  $G_t$  remains well defined, it is usually assumed that all policies are proper (Bertsekas and Tsitsiklis, 1996), i.e., for any policy  $\pi$ , the chain induced by  $\pi$  has some absorbing states, one of which the agent will eventually go to with probability 1. Furthermore, the rewards are always 0 thereafter. For any  $\gamma \in [0, 1]$ ,  $G_0$  is the random variable indicating the total reward, and we use its expectation

$$J(\pi) \doteq \mathbb{E}_{\mu_0, p, \pi}[G_0],$$

as our primary performance metric. In particular, when  $\gamma = 1$ , we can express  $G_0$  as  $G_0 = \sum_{t=0}^{T-1} r(S_t, A_t)$ , where  $T$  is a random variable indicating the first time the agent goes to an absorbing state. For any  $\gamma \in [0, 1]$ , the state value function and the state-action value function are defined as  $v_{\pi}(s) \doteq \mathbb{E}[G_t | S_t = s]$  and  $q_{\pi}(s, a) \doteq \mathbb{E}[G_t | S_t = s, A_t = a]$  respectively.

**Total Reward Perspective.** Previous mean-variance RL methods (Prashanth and Ghavamzadeh, 2013; Tamar et al., 2012; Xie et al., 2018) usually consider the variance of the total reward. Namely, they consider the following problem:

$$\max_{\theta} \mathbb{E}[G_0] \quad \text{subject to} \quad \mathbb{V}(G_0) \leq \xi, \quad (1)$$

where  $\mathbb{V}(\cdot)$  indicates the variance of a random variable,  $\xi$  indicates the user's tolerance for variance, and  $\pi$  is parameterized by  $\theta$ . In particular, Prashanth and Ghavamzadeh (2013) consider the setting  $\gamma < 1$  and convert (1) into an unconstrained saddle-point problem:  $\max_{\lambda} \min_{\theta} L_1(\theta, \lambda) \doteq -\mathbb{E}[G_0] + \lambda(\mathbb{V}(G_0) - \xi)$ , where  $\lambda$  is the dual variable. Prashanth and Ghavamzadeh (2013) use stochastic gradient descent to find the saddle-point of  $L_1(\theta, \lambda)$ . To estimate  $\nabla_{\theta, \lambda} L_1(\theta, \lambda)$ , they propose two simultaneous perturbation methods: simultaneous perturbation

stochastic approximation and smoothed functional (Bhatnagar et al., 2013), yielding a three-timescale algorithm. Empirical success is observed in a simple traffic control MDP.

Tamar et al. (2012) consider the setting  $\gamma = 1$ . Instead of using the saddle-point formulation in Prashanth and Ghavamzadeh (2013), they consider the following unconstrained problem:  $\max_{\theta} L_2(\theta) \doteq \mathbb{E}[G_0] - \lambda g(\mathbb{V}(G_0) - \xi)$ , where  $\lambda > 0$  is a hyperparameter to be tuned and  $g(\cdot)$  is a penalty function, which they define as  $g(x) \doteq (\max\{0, x\})^2$ . The analytical expression of  $\nabla_{\theta} L_2(\theta)$  they provide involves a term  $\mathbb{E}[G_0] \nabla_{\theta} \mathbb{E}[G_0]$ , leading to a double sampling issue. To address this, Tamar et al. (2012) consider a two-timescale algorithm and keep running estimates for  $\mathbb{E}[G_0]$  and  $\mathbb{V}[G_0]$  in a faster timescale, yielding an episodic algorithm. Empirical success is observed in a simple portfolio management MDP.

Xie et al. (2018) consider the setting  $\gamma = 1$  and set the penalty function  $g(\cdot)$  in Tamar et al. (2012) to the identity function. To address the double sampling issue in Tamar et al. (2012), they exploit the Fenchel duality  $x^2 = \max_y (2xy - y^2)$ , yielding the following problem:  $\max_{\theta, y} L_3(\theta, y) \doteq 2y(\mathbb{E}[G_0] + \frac{1}{2\lambda}) - y^2 - \mathbb{E}[G_0^2]$ , where  $y$  is the dual variable. Xie et al. (2018) then propose a solver based on stochastic coordinate ascent, yielding an episodic algorithm.

**Per-Step Reward Perspective.** Recently Bisi et al. (2019) propose a reward-volatility risk measure, which is the variance of a per-step reward random variable  $R$ . In the setting  $\gamma < 1$ , it is well known that the expected total discounted reward can be expressed as

$$J(\pi) = \frac{1}{1-\gamma} \sum_{s,a} d_{\pi}(s,a) r(s,a),$$

where  $d_{\pi}(s,a)$  is the normalized discounted state-action distribution:

$$d_{\pi}(s,a) \doteq (1-\gamma) \sum_{t=0}^{\infty} \gamma^t \Pr(S_t = s, A_t = a | \mu_0, \pi, p).$$

We now define the per-step reward random variable  $R$ , a discrete random variable taking values in the image of  $r$ , by defining its probability mass function as  $p(R = x) = \sum_{s,a} d_{\pi}(s,a) \mathbb{I}_{r(s,a)=x}$ , where  $\mathbb{I}$  is the indicator function. It follows that  $\mathbb{E}[R] = (1-\gamma)J(\pi)$ . Bisi et al. (2019) argue that  $\mathbb{V}(R)$  can better capture short-term risk than  $\mathbb{V}(G_0)$ . Furthermore, Bisi et al. (2019) show that  $\mathbb{V}(G_0) \leq \frac{\mathbb{V}(R)}{(1-\gamma)^2}$ , indicating that minimizing the variance of  $R$  implicitly minimizes the variance of  $G_0$ . Bisi et al. (2019), therefore, consider the following problem:  $J_{\lambda}(\pi) \doteq \mathbb{E}[R] - \lambda \mathbb{V}(R) = \mathbb{E}[R - \lambda(R - \mathbb{E}[R])^2]$ . In other words, to optimize the risk-aware objective  $J_{\lambda}(\pi)$  is to optimize the canonical risk-neutral objective of a new MDP, which is the same as the original MDP except that the new reward function is  $r'(s,a) \doteq r(s,a) - \lambda(r(s,a) - (1-\gamma)J(\pi))^2$ . However, there are two challenges with this formulation, as pointed out by Bisi et al. (2019). The first challenge comes from the new reward function  $r'$ , which depends on the policy  $\pi$  due to the occurrence of  $J(\pi)$ . By contrast, in the canonical RL setting (Puterman, 2014; Sutton and Barto, 2018), the reward function  $r$  does not depend on  $\pi$ . We refer to this as the *policy-dependent-reward issue*. Due to this issue, the rich classical MDP toolbox cannot be applied to this new MDP easily, and Bisi et al. (2019) do not work on this new MDP directly. They instead derive a policy gradient for  $J_{\lambda}(\pi)$  directly. The second challenge then arises in computing the policy gradient. To obtain an unbiased gradient estimator, three independent sets of samples are required, which we refer to as the *triple-sampling issue*. Bisi et al. (2019) also propose Trust Region Volatility Optimization (TRVO), for optimizing  $J_{\lambda}(\pi)$  based on a variant of the performance difference theorem (Kakade and Langford, 2002).

We argue that the variance of the per-step reward is easier to optimize than the variance of the total reward. The methods of Tamar et al. (2012); Xie et al. (2018) involve terms like  $(\mathbb{E}[G_0])^2$  and  $\mathbb{E}[G_0^2]$ , which lead to terms like  $G_0^2 \sum_{t=0}^{T-1} \nabla_{\theta} \log \pi(A_t | S_t)$  in their update rules, yielding large variance. In particular, it is computationally prohibitive to further expand  $G_0^2$  explicitly to apply variance reduction techniques like baselines (Williams, 1992). By contrast, we show in the next section that MVPI involves only  $r(s,a)^2$ , which is easier to deal with than  $G_0^2$ .

### 3 Mean-Variance Policy Iteration

Although in many problems our goal is to maximize the expected total undiscounted reward, practitioners often find that optimizing the discounted objective ( $\gamma < 1$ ) as a proxy for the undiscounted objective ( $\gamma = 1$ ) is better than optimizing the undiscounted objective directly, especially when deep neural networks are used as function approximators (Mnih et al., 2015; Lillicrap et al., 2015; Espeholt

et al., 2018; Xu et al., 2018; Van Seijen et al., 2019). We, therefore, focus on the discounted setting in the paper, which allows us to consider the per-step reward perspective.

Although the aforementioned policy-dependent-reward and triple-sampling issues look separate, we offer a unified solution to fix both simultaneously. We use the Fenchel duality to rewrite  $J_\lambda(\pi)$  as

$$J_\lambda(\pi) = \mathbb{E}[R] - \lambda\mathbb{E}[R^2] + \lambda(\mathbb{E}[R])^2 = \mathbb{E}[R] - \lambda\mathbb{E}[R^2] + \lambda \max_y (2\mathbb{E}[R]y - y^2), \quad (2)$$

yielding the following problem:

$$\max_{\pi, y} J_\lambda(\pi, y) \doteq \sum_{s, a} d_\pi(s, a)(r(s, a) - \lambda r(s, a)^2 + 2\lambda r(s, a)y) - \lambda y^2. \quad (3)$$

We propose a *block cyclic coordinate ascent* (BCCA, Luenberger and Ye 1984; Tseng 2001; Saha and Tewari 2010, 2013; Wright 2015) framework to solve (3), which updates  $y$  and  $\pi$  alternatively as shown in Algorithm 1. At the  $k$ -th iteration, we first fix  $\pi_k$  and update  $y_{k+1}$  (Step 1). As  $J_\lambda(\pi_k, y)$  is

---

**Algorithm 1:** Mean-Variance Policy Iteration (MVPI)

---

```

for  $k = 1, \dots$  do
  Step 1:  $y_{k+1} \doteq (1 - \gamma)J(\pi_k)$  // The exact solution for  $\arg \max_y J_\lambda(\pi_k, y)$ 
  Step 2:  $\pi_{k+1} \doteq \arg \max_\pi \left( \sum_{s, a} d_\pi(s, a)(r(s, a) - \lambda r(s, a)^2 + 2\lambda r(s, a)y_{k+1}) - \lambda y_{k+1}^2 \right)$ 
end

```

---

quadratic in  $y$ ,  $y_{k+1}$  can be computed analytically as  $y_{k+1} = \sum_{s, a} d_{\pi_k}(s, a)r(s, a) = (1 - \gamma)J(\pi_k)$ , i.e., all we need in this step is  $J(\pi_k)$ , which is exactly the performance metric of the policy  $\pi_k$ . We, therefore, refer to Step 1 as *policy evaluation*. We then fix  $y_{k+1}$  and update  $\pi_{k+1}$  (Step 2). Remarkably, Step 2 can be reduced to the following problem:

$$\pi_{k+1} = \arg \max_\pi \sum_{s, a} d_\pi(s, a)\hat{r}(s, a; y_{k+1}),$$

where  $\hat{r}(s, a; y) \doteq r(s, a) - \lambda r(s, a)^2 + 2\lambda r(s, a)y$ . In other words, to compute  $\pi_{k+1}$ , we need to solve a new MDP, which is the same as the original MDP except that the reward function is  $\hat{r}$  instead of  $r$ . This new reward function  $\hat{r}$  does not depend on the policy  $\pi$ , avoiding the policy-dependent-reward issue of Bisi et al. (2019). In this step, a new policy  $\pi_{k+1}$  is computed. An intuitive conjecture is that this step is a *policy improvement* step, and we confirm this with the following theorem:

**Theorem 1.** (*Monotonic Policy Improvement*)  $\forall k, J_\lambda(\pi_{k+1}) \geq J_\lambda(\pi_k)$ .

Though the monotonic improvement w.r.t. the objective  $J_\lambda(\pi, y)$  in Eq (3) follows directly from standard BCCA theory, Theorem 1 provides the monotonic improvement w.r.t. the objective  $J_\lambda(\pi)$  in Eq (2). The proof is provided in the appendix. Given Theorem 1, we can now consider the whole BCCA framework in Algorithm 1 as a policy iteration framework, which we call *mean-variance policy iteration* (MVPI). Let  $\{\pi_\theta : \theta \in \Theta\}$  be the function class for policy optimization. We make standard assumptions on the policy parameterization (e.g., see Assumption 4.1 in Papini et al. (2018)):

**Assumption 1.**  $\sup_{\theta \in \Theta} \left\| \frac{\partial \log \pi_\theta(a|s)}{\partial \theta_i \partial \theta_j} \right\| < \infty, \sup_{\theta \in \Theta} \left\| \nabla_\theta \log \pi_\theta(a|s) \right\| < \infty$ , and  $\Theta$  is compact.

**Theorem 2.** (*Convergence of MVPI with function approximation*) Under Assumption 1, let

$$y_{k+1} \doteq \arg \max_y J_\lambda(\theta_k, y), \quad \theta_{k+1} \doteq \arg \max_{\theta \in \Theta} J_\lambda(\theta, y_{k+1}),$$

then  $J_\lambda(\theta_{k+1}) \geq J_\lambda(\theta_k)$ ,  $\{J_\lambda(\theta_k)\}_{k=1, \dots}$  converges, and  $\lim_{k \rightarrow \infty} \left\| \nabla_\theta J_\lambda(\theta_k) \right\| = 0$ .

The proof is provided in the appendix. MVPI enjoys great flexibility in that any policy evaluation method and risk-neutral control method can be dropped in off the shelf, which makes it possible to leverage all the advances in risk-neutral RL. MVPI differs from the standard policy iteration (PI, e.g., see Bertsekas and Tsitsiklis (1996); Puterman (2014); Sutton and Barto (2018)) in two key ways: (1) policy evaluation in MVPI requires only a scalar performance metric, while standard policy evaluation involves computing the value of all states. (2) policy improvement in MVPI considers an augmented reward  $\hat{r}$ , which is different at each iteration, while standard policy improvement always considers the original reward. Standard PI can be used to solve the policy improvement step in MVPI.

### 3.1 Average Reward Setting

So far we have considered the total reward as the primary performance metric for mean-variance RL. We now show that MVPI can also be used when we consider the average reward as the primary performance metric. Assuming the chain induced by  $\pi$  is ergodic and letting  $\bar{d}_\pi(s)$  be its stationary distribution, Filar et al. (1989); Prashanth and Ghavamzadeh (2013) consider the *long-run variance* risk measure  $\Lambda(\pi) \doteq \sum_{s,a} \bar{d}_\pi(s,a) (r(s,a) - \bar{J}(\pi))^2$  for the average reward setting, where  $\bar{d}_\pi(s,a) \doteq \bar{d}_\pi(s)\pi(a|s)$  and  $\bar{J}(\pi) = \sum_{s,a} \bar{d}_\pi(s,a)r(s,a)$  is the average reward. We now define a risk-aware objective

$$\bar{J}_\lambda(\pi) \doteq \bar{J}(\pi) - \lambda\Lambda(\pi) = \max_y \sum_{s,a} \bar{d}_\pi(s,a)\hat{r}(s,a;y) - \lambda y^2, \quad (4)$$

where we have used the Fenchel duality and BCCA can take over to derive MVPI for the average reward setting as Algorithm 1. It is not a coincidence that the only difference between (3) and (4) is the difference between  $d_\pi$  and  $\bar{d}_\pi$ . The root cause is that the total discounted reward of an MDP is always equivalent to the average reward of an artificial MDP (up to a constant multiplier), whose transition kernel is  $\tilde{p}(s'|s,a) = \gamma p(s'|s,a) + (1-\gamma)\mu_0(s')$  (e.g., see Section 2.4 in Konda (2002) for details).

### 3.2 Off-Policy Learning

Previous mean-variance RL methods from the total reward perspective consider only the on-policy setting and cannot be easily extended to the off-policy setting. For example, it is not clear whether perturbation methods for estimating gradients (Prashanth and Ghavamzadeh, 2013) can be used off-policy. To reweight terms like  $G_0^2 \sum_{t=0}^{T-1} \nabla_\theta \log \pi(A_t|S_t)$  from Tamar et al. (2012); Xie et al. (2018) in the off-policy setting, we would need to compute the product of importance sampling ratios  $\prod_{i=0}^{T-1} \frac{\pi(a_i|s_i)}{\mu(a_i|s_i)}$ , where  $\mu$  is the behavior policy. This product usually suffers from high variance (Precup et al., 2001; Liu et al., 2018) and requires knowing the behavior policy  $\mu$ , both of which are practical obstacles in real applications.

We consider MVPI in both on-line and off-line off-policy settings. In the on-line off-policy setting, an agent interacts with the environment following a behavior policy  $\mu$  to collect transitions, which are stored into a replay buffer (Lin, 1992) for future reuse. Mujoco robot simulation tasks (Brockman et al., 2016) are common benchmarks for this paradigm (Lillicrap et al., 2015; Haarnoja et al., 2018), and TD3 is a leading algorithm in Mujoco tasks (Achiam, 2018). TD3 is a risk-neutral control algorithm, reducing the over-estimation bias (Hasselt, 2010) of DDPG (Lillicrap et al., 2015), which is a neural network implementation of the deterministic policy gradient theorem (Silver et al., 2014). Given the empirical success of TD3, we propose MVPI-TD3 for risk-averse control this setting. In the policy evaluation step of MVPI-TD3, we set  $y_{k+1}$  to the average of the recent  $K_1$  rewards, assuming the policy changes slowly. Theoretically, we should use a weighted average as  $d_\pi(s,a)$  is a discounted distribution. Though implementing this weighted average is straightforward, practitioners usually ignore discounting for state visitation in policy gradient methods to improve sample efficiency (Mnih et al., 2016; Schulman et al., 2015, 2017; Bacon et al., 2017). Hence, we do not use the weighted average in MVPI-TD3. In the policy improvement step of MVPI-TD3, we sample a mini-batch of transitions from the replay buffer and perform one TD3 gradient update. The pseudocode of MVPI-TD3 is provided in the appendix.

In the off-line off-policy setting, we are presented with a batch of transitions  $\{s_i, a_i, r_i, s'_i\}_{i=1,\dots,K}$  and want to learn a good target policy  $\pi$  for control solely from this batch of transitions. Sometimes those transitions are generated by following a known behavior policy  $\mu$ . But more commonly, those transitions are generated from multiple unknown behavior policies, which we refer to as the behavior-agnostic off-policy setting (Nachum et al., 2019a). Namely, the state-action pairs  $(s_i, a_i)$  are distributed according to some unknown distribution  $d$ , which may result from multiple unknown behavior policies. The successor state  $s'_i$  is distributed according to  $p(\cdot|s_i, a_i)$  and  $r_i = r(s, a)$ . The degree of off-policiness in this setting is usually larger than the on-line off-policy setting.

In the off-line off-policy setting, the policy evaluation step in MVPI becomes the standard *off-policy evaluation* problem (Thomas et al., 2015; Thomas and Brunskill, 2016; Jiang and Li, 2016; Liu et al., 2018), where we want to estimate a scalar performance metric of a policy with off-line samples. One promising approach to off-policy evaluation is *density ratio learning*, where we use function

approximation to learn the density ratio  $\frac{d_\pi(s, a)}{d(s, a)}$  directly (Hallak and Manner, 2017; Liu et al., 2018; Gelada and Bellemare, 2019; Nachum et al., 2019a; Zhang et al., 2020a,b; Mousavi et al., 2020), which we then use to reweight  $r(s, a)$ . All those off-policy evaluation algorithms can be integrated into MVPI in a plug-and-play manner. In the off-line off-policy setting, the policy improvement step in MVPI becomes the standard *off-policy policy optimization* problem, where we can reweight the canonical on-policy actor-critic (Sutton et al., 2000; Konda, 2002) with the density ratio as in Liu et al. (2019) to achieve off-policy policy optimization. Algorithm 2 provides an example of Off-line MVPI.

---

**Algorithm 2:** Off-line MVPI

---

**Input:** A batch of transitions  $\{s_i, a_i, r_i, s'_i\}_{i=1, \dots, K}$  and a learning rate  $\alpha$

**while** *True* **do**

- Learn the density ratio  $\rho_\pi(s, a) \doteq \frac{d_\pi(s, a)}{d(s, a)}$  with  $\{s_i, a_i, r_i, s'_i\}_{i=1, \dots, K}$
- // For example, use DualDICE (Nachum et al., 2019a)
- $y \leftarrow \frac{1}{K} \sum_{i=1}^K \rho_\pi(s_i, a_i) r_i$
- for**  $i = 1, \dots, K$  **do**
- $\hat{r}_i \leftarrow r_i - \lambda r_i^2 + 2\lambda r_i y$
- $a'_i \sim \pi(\cdot | s'_i)$
- end**
- Learn  $q_\pi(s, a)$  with  $\{s_i, a_i, \hat{r}_i, s'_i, a'_i\}_{i=1, \dots, K}$
- // For example, use TD(0) (Sutton, 1988) in  $\mathcal{S} \times \mathcal{A}$
- $\theta \leftarrow \theta + \alpha \rho_\pi(s_i, a_i) \nabla_\theta \log \pi(a_i | s_i) q_\pi(s_i, a_i)$ , where  $i$  is randomly selected

**end**

---

## 4 Experiments

**On-Line Off-Policy Setting.** In many real-world robot applications, e.g., in a warehouse, it is crucial that the robots’ performance be consistent. In such cases, risk-averse RL is an appealing option to train robots. Motivated by this, we benchmark MVPI-TD3 on eight Mujoco robot manipulation tasks from OpenAI gym. As we are not aware of any other off-policy mean-variance RL method, we use several recent on-policy mean-variance RL method as baselines, namely, the methods of Tamar et al. (2012); Prashanth and Ghavamzadeh (2013), MVP (Xie et al., 2018), and TRVO (Bisi et al., 2019). The methods of Tamar et al. (2012); Prashanth and Ghavamzadeh (2013) and MVP are not designed for deep RL settings. To make the comparison fair, we improve those baselines with multiple parallel actors to stabilize the training of neural networks as in Mnih et al. (2016).<sup>2</sup> TRVO is essentially plugging in TRPO into MVPI for the policy improvement. We, therefore, implement TRVO as MVPI with Proximal Policy Optimization (PPO, Schulman et al. 2017) to improve its performance. We also use the vanilla risk-neutral TD3 as a baseline. We use two-hidden-layer neural networks for function approximation.

We run each algorithm for  $10^6$  steps and evaluate the algorithm every  $10^4$  steps for 20 episodes. We report the mean of those 20 episodic returns against the training steps in Figure 1. The curves are generated by setting  $\lambda = 1$ . More details are provided in the appendix. The results show that MVPI-TD3 outperforms all risk-averse baselines in all tested domains (in terms of both final episodic return and learning speed), with only one exception, InvertedDoublePendulum, where TRVO outperforms MVPI-TD3. Moreover, the curves of the methods from the total reward perspective are always flat in all domains with only one exception that MVP achieves a reasonable performance in Reacher, though exhaustive hyperparameter tuning is conducted, including  $\lambda$  and  $\xi$ . Those results suggest that perturbation-based gradient estimation in Prashanth and Ghavamzadeh (2013) may not work well with neural networks, and the  $G_0^2 \sum_{t=0}^{T-1} \nabla_\theta \log \pi(a_t | s_t)$  term in Tamar et al. (2012) and MVP suffers from high variance, yielding instability. By contrast, the two algorithms from the per-step reward perspective (MVPI-TD3 and TRVO) do learn a reasonable policy.

<sup>2</sup>They are on-policy algorithms so we cannot use experience replay.

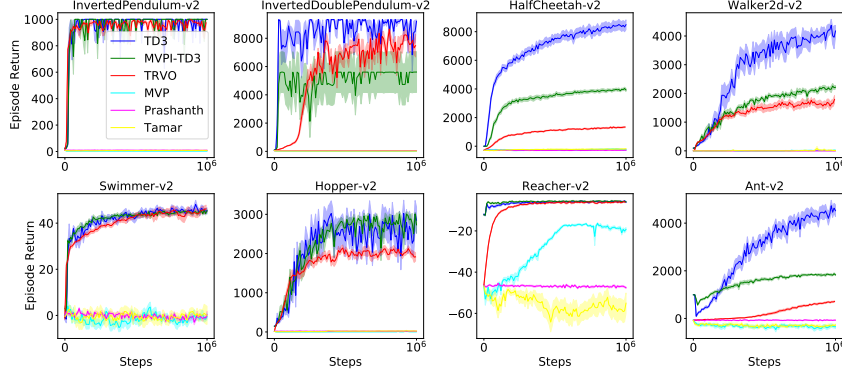


Figure 1: Training progress of MVPI-TD3 and baseline algorithms. Curves are averaged over 10 independent runs with shaded regions indicating standard errors.

As shown in Figure 1, the vanilla risk-neutral TD3 outperforms all risk-averse algorithms (in terms of episodic return). This is expected as it is in general hard for a risk-averse algorithm to outperform its risk-neutral counterpart in terms of a risk-neutral performance metric. We now compare TD3, MVPI-TD3 and TRVO in terms of a risk-aware performance metric. To this end, we test the agent at the end of training for an extra 100 episodes to compute a risk-aware performance metric. We report the normalized statistics in Table 1. The results show that MVPI-TD3 outperforms TD3 in 6 out of 8 tasks in terms of the risk-aware performance metric. Moreover, MVPI-TD3 outperforms TRVO in 6 out of 8 tasks. This performance boost of MVPI-TD3 over TRVO indeed results from the performance boost of TD3 over PPO, and it is the flexibility of MVPI that makes this off-the-shelf application TD3 in risk-averse RL possible. We also provide versions of Figure 1 and Table 1 with  $\lambda = 0.5$  and  $\lambda = 2$  in the appendix. The relative performance is the same as  $\lambda = 1$ .

	$\Delta_{\text{J}}^{\text{TRVO}}$	$\Delta_{\text{mean}}^{\text{TRVO}}$	$\Delta_{\text{variance}}^{\text{TRVO}}$	$\Delta_{\text{J}}^{\text{MVPI-TD3}}$	$\Delta_{\text{mean}}^{\text{MVPI-TD3}}$	$\Delta_{\text{variance}}^{\text{MVPI-TD3}}$
InvertedPendulum	-1107%	-3%	$10^8\%$ <sup>3</sup>	0%	0%	0%
InvertedDoubleP.	-1915%	-27%	1867%	82%	-40%	-81%
HalfCheetah	82%	-84%	-83%	86%	-53%	-85%
Walker2d	36%	-61%	-36%	97%	-47%	-97%
Swimmer	-5%	0%	190%	-5%	0%	153%
Hopper	26%	-31%	-26%	84%	-6%	-84%
Reacher	-42%	-7%	87%	2%	5%	2%
Ant	98%	-84%	-98%	98%	-59%	-98%

Table 1: Normalized statistics of TRVO and MVPI-TD3. For  $\text{algo} \in \{\text{MVPI-TD3}, \text{TRVO}, \text{TD3}\}$ , we compute the risk-aware performance metric as  $J_{\text{algo}} \doteq \text{mean}_{\text{algo}} - \lambda \text{variance}_{\text{algo}}$  with  $\lambda = 1$ , where  $\text{mean}_{\text{algo}}$  and  $\text{variance}_{\text{algo}}$  are computed from the 100 evaluation episodic returns. Then we compute the normalized statistics as  $\Delta_{\text{J}}^{\text{algo}} \doteq \frac{J_{\text{algo}} - J_{\text{TD3}}}{|J_{\text{TD3}}|}$ ,  $\Delta_{\text{mean}}^{\text{algo}} \doteq \frac{\text{mean}_{\text{algo}} - \text{mean}_{\text{TD3}}}{|\text{mean}_{\text{TD3}}|}$ ,  $\Delta_{\text{perf}}^{\text{algo}} \doteq \frac{\text{variance}_{\text{algo}} - \text{variance}_{\text{TD3}}}{|\text{variance}_{\text{TD3}}|}$ . Both MVPI-TD3 and TRVO are trained with  $\lambda = 1$ . All  $J_{\text{algo}}$  are averaged over 10 independent runs.

**Off-Line Off-Policy Setting.** We consider an infinite horizon MDP (Figure 2a). Two actions  $a_0$  and  $a_1$  are available at  $s_0$ , and we have  $p(s_3|s_0, a_1) = 1, p(s_1|s_0, a_0) = p(s_2|s_0, a_0) = 0.5$ . The discount factor is  $\gamma = 0.7$  and the agent is initialized at  $s_0$ . We consider the objective  $J_{\lambda}(\pi)$  in Eq (2). If  $\lambda = 0$ , the optimal policy is to choose  $a_0$ . If  $\lambda$  is large enough, the optimal policy is to choose  $a_1$ . We consider the behavior-agnostic off-policy setting, where the sampling distribution  $d$  satisfies  $d(s_0, a_0) = d(s_0, a_1) = d(s_1) = d(s_2) = d(s_3) = 0.2$ . This sampling distribution may result from multiple unknown behavior policies. Although the representation is tabular, we use a softmax policy. So the problem we consider is nonlinear and nonconvex. As we are not aware of any other behavior-agnostic off-policy risk-averse RL method, we benchmark only Off-line MVPI (Algorithm 2). Details are provided in the appendix. We report the probability of selecting  $a_0$  against

<sup>3</sup>This is an overflow. Both the policy from TD3 and the environment are deterministic. So the variance of the TD3 evaluation episodic returns is 0.

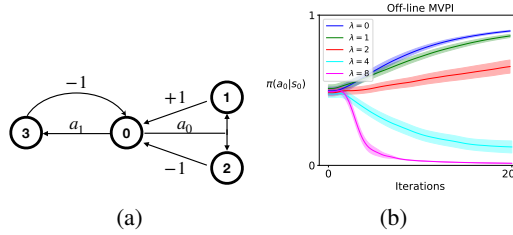


Figure 2: (a) A tabular MDP. (b) The training progress of Off-line MVPI. Curves are averaged over 30 independent runs with shaded regions indicating standard errors.

training iterations. As shown in Figure 2b,  $\pi(a_0|s_0)$  decreases as  $\lambda$  increases, indicating Off-line MVPI copes well with different risk levels. The main challenge in Off-line MVPI rests on learning the density ratio. Scaling up density ratio learning algorithms reliably to more challenging domains like Mujoco is out of the scope of this paper.

## 5 Related Work

Both MVPI and Bisi et al. (2019) consider the per-step reward perspective for mean-variance RL. To the best of our knowledge, MVPI is the first to enable dropping in any off-the-shelf risk-neutral RL method for risk-averse RL. In particular, MVPI addresses two bottlenecks of Bisi et al. (2019), i.e., the triple-sampling issue and the policy-dependent reward issue. In particular, MVPI adopts deterministic policies (Silver et al., 2014) and off-policy training easily. Deterministic policies play an important role in reducing the variance of a policy (Silver et al., 2014). Off-policy learning is important for improving data efficiency (Mnih et al., 2015) and exploration (Osband et al., 2018). Both, to the best of our knowledge, have not explored in the risk-averse RL literature. Enabling deterministic policies and off-policy learning in Bisi et al. (2019) may require algorithm-specific adaptations to existing risk-neutral methods and is not explored in Bisi et al. (2019). Furthermore, MVPI works for both the total discounted reward setting and the average reward setting. It is not clear how the performance difference lemma in Bisi et al. (2019), which plays a central role in TRVO, can be adapted to the average reward setting.

Besides variance, value at risk (VaR, Chow et al. 2018), conditional value at risk (CVaR, Chow and Ghavamzadeh 2014; Tamar et al. 2015; Chow et al. 2018), sharp ratio (Tamar et al., 2012), and exponential utility (Howard and Matheson, 1972; Borkar, 2002) are also used for risk-averse RL. In particular, it is straightforward to consider exponential utility for the per-step reward, which, however, suffers from the same problems as the exponential utility for the total reward (Gosavi et al., 2014), e.g., it overflows easily.

## 6 Conclusion

In this paper, we propose MVPI for risk-averse RL. MVPI enjoys great flexibility such that any policy evaluation method and risk-neutral control method can be dropped in for risk-averse control off the shelf, in both on- and off-policy settings. To the best of our knowledge, MVPI is the first empirical success of risk-averse RL in Mujoco robot simulation domains, and is also the first success of off-policy risk-averse RL. Possibilities for future work include considering other risk measures (e.g., VaR and CVaR) of the per-step reward random variable, integrating more advanced off-policy policy optimization techniques (e.g., Nachum et al. 2019b) in off-policy MVPI, optimizing  $\lambda$  with meta-gradients (Xu et al., 2018), conducting a sample complexity analysis for MVPI, and developing theories for approximate MVPI.

## Broader Impact

Risk-averse RL has many potential real-world applications, e.g., pricing (Wang, 2000), healthcare (Parker, 2009), portfolio management (Lai et al., 2011), autonomous driving (Matthaeia et al., 2015),

and robotics (Majumdar and Pavone, 2020). Our work makes it possible to leverage advances in risk-neutral RL for risk-averse RL easily. In particular, with our framework, an autonomous driving car may become safer, a patient may suffer less from medical accidents, a portfolio manager may control her portfolio’s risk, and a policymaker may reduce the risk of international conflicts.

Like many other RL agents, agents trained with our framework are also vulnerable to adversarial attacks. This means the users, e.g., companies or governments, should take extra care for such attacks when deploying the learned agents in the real world. Otherwise, they may suffer from property losses. Like any other RL system, to make use of our proposed framework, an environment must be provided, which is usually a simulator. If the simulator is biased or unfair, it is likely that the agents from our framework will also be biased or unfair. Also, the performance of the agent in the simulator may not faithfully reflect the deploy-time performance of the agent, due to unavoidable differences between a simulator and the real world. Our proposed framework considers a stationary environment, so the agent may not be able to cope well with nonstationary scenarios, which are common in the real world. In principle, our proposed framework does not raise any privacy issues. However, to make a better simulator, users may be tempted to exploit personal data. To address those issues, it is beneficial to have institutes to certify an RL agent, in terms of, e.g., fairness or security, before it is allowed to be deployed in the real world. Like any artificial intelligence system, our proposed framework has the potential to greatly improve human productivity. However, it may also reduce the need for human workers, resulting in job losses.

## Acknowledgments and Disclosure of Funding

SZ is generously funded by the Engineering and Physical Sciences Research Council (EPSRC). This project has received funding from the European Research Council under the European Union’s Horizon 2020 research and innovation programme (grant agreement number 637713). The experiments were made possible by a generous equipment grant from NVIDIA. BL’s research is funded by the National Science Foundation (NSF) under grant NSF IIS1910794 and an Amazon Research Award.

## References

Achiam, J. (2018). Spinning up in deep reinforcement learning.

Bacon, P.-L., Harb, J., and Precup, D. (2017). The option-critic architecture. In *Proceedings of the 31st AAAI Conference on Artificial Intelligence*.

Bertsekas, D. (1995). *Nonlinear Programming*. Athena Scientific.

Bertsekas, D. P. and Tsitsiklis, J. N. (1996). *Neuro-Dynamic Programming*. Athena Scientific Belmont, MA.

Bhatnagar, S., Prasad, H., and Prashanth, L. (2013). *Stochastic Recursive Algorithms for Optimization*. Springer London.

Bisi, L., Sabbioni, L., Vittori, E., Papini, M., and Restelli, M. (2019). Risk-averse trust region optimization for reward-volatility reduction. *arXiv preprint arXiv:1912.03193*.

Borkar, V. S. (2002). Q-learning for risk-sensitive control. *Mathematics of operations research*.

Brockman, G., Cheung, V., Pettersson, L., Schneider, J., Schulman, J., Tang, J., and Zaremba, W. (2016). Openai gym. *arXiv preprint arXiv:1606.01540*.

Chow, Y. (2017). *Risk-Sensitive and Data-Driven Sequential Decision Making*. PhD thesis, Stanford University.

Chow, Y. and Ghavamzadeh, M. (2014). Algorithms for cvar optimization in mdps. In *Advances in Neural Information Processing Systems*.

Chow, Y., Ghavamzadeh, M., Janson, L., and Pavone, M. (2018). Risk-constrained reinforcement learning with percentile risk criteria. *The Journal of Machine Learning Research*.

Dhariwal, P., Hesse, C., Klimov, O., Nichol, A., Plappert, M., Radford, A., Schulman, J., Sidor, S., Wu, Y., and Zhokhov, P. (2017). Openai baselines. <https://github.com/openai/baselines>.

Espeholt, L., Soyer, H., Munos, R., Simonyan, K., Mnih, V., Ward, T., Doron, Y., Firoiu, V., Harley, T., Dunning, I., et al. (2018). Impala: Scalable distributed deep-rl with importance weighted actor-learner architectures. *arXiv preprint arXiv:1802.01561*.

Filar, J. A., Kallenberg, L. C., and Lee, H.-M. (1989). Variance-penalized markov decision processes. *Mathematics of Operations Research*.

Fujimoto, S., van Hoof, H., and Meger, D. (2018). Addressing function approximation error in actor-critic methods. *arXiv preprint arXiv:1802.09477*.

Gelada, C. and Bellemare, M. G. (2019). Off-policy deep reinforcement learning by bootstrapping the covariate shift. In *Proceedings of the 33rd AAAI Conference on Artificial Intelligence*.

Gosavi, A. A., Das, S. K., and Murray, S. L. (2014). Beyond exponential utility functions: A variance-adjusted approach for risk-averse reinforcement learning. In *2014 IEEE Symposium on Adaptive Dynamic Programming and Reinforcement Learning*.

Haarnoja, T., Zhou, A., Abbeel, P., and Levine, S. (2018). Soft actor-critic: Off-policy maximum entropy deep reinforcement learning with a stochastic actor. *arXiv preprint arXiv:1801.01290*.

Hallak, A. and Mannor, S. (2017). Consistent on-line off-policy evaluation. In *Proceedings of the 34th International Conference on Machine Learning*.

Hasselt, H. V. (2010). Double q-learning. In *Advances in neural information processing systems*.

Howard, R. A. and Matheson, J. E. (1972). Risk-sensitive markov decision processes. *Management Science*.

Jiang, N. and Li, L. (2016). Doubly robust off-policy value evaluation for reinforcement learning. In *International Conference on Machine Learning*.

Kakade, S. and Langford, J. (2002). Approximately optimal approximate reinforcement learning. In *Proceedings of the 19th International Conference on Machine Learning*.

Konda, V. R. (2002). *Actor-critic algorithms*. PhD thesis, Massachusetts Institute of Technology.

Lai, T. L., Xing, H., Chen, Z., et al. (2011). Mean-variance portfolio optimization when means and covariances are unknown. *The Annals of Applied Statistics*.

Li, D. and Ng, W.-L. (2000). Optimal dynamic portfolio selection: Multiperiod mean-variance formulation. *Mathematical finance*.

Lillicrap, T. P., Hunt, J. J., Pritzel, A., Heess, N., Erez, T., Tassa, Y., Silver, D., and Wierstra, D. (2015). Continuous control with deep reinforcement learning. *arXiv preprint arXiv:1509.02971*.

Lin, L.-J. (1992). Self-improving reactive agents based on reinforcement learning, planning and teaching. *Machine Learning*.

Liu, Q., Li, L., Tang, Z., and Zhou, D. (2018). Breaking the curse of horizon: Infinite-horizon off-policy estimation. In *Advances in Neural Information Processing Systems*.

Liu, Y., Swaminathan, A., Agarwal, A., and Brunskill, E. (2019). Off-policy policy gradient with state distribution correction. *arXiv preprint arXiv:1904.08473*.

Luenberger, D. G. and Ye, Y. (1984). *Linear and nonlinear programming (3rd Edition)*. Springer.

Maei, H. R. (2011). *Gradient temporal-difference learning algorithms*. PhD thesis, University of Alberta.

Majumdar, A. and Pavone, M. (2020). How should a robot assess risk? towards an axiomatic theory of risk in robotics. In *Robotics Research*. Springer.

Mannor, S. and Tsitsiklis, J. (2011). Mean-variance optimization in markov decision processes. *arXiv preprint arXiv:1104.5601*.

Markowitz, H. M. and Todd, G. P. (2000). *Mean-variance analysis in portfolio choice and capital markets*. John Wiley & Sons.

Matthaeia, R., Reschkaa, A., Riekena, J., Dierkesa, F., Ulbricha, S., Winkleb, T., and Maurera, M. (2015). Autonomous driving: Technical, legal and social aspects.

Mnih, V., Badia, A. P., Mirza, M., Graves, A., Lillicrap, T., Harley, T., Silver, D., and Kavukcuoglu, K. (2016). Asynchronous methods for deep reinforcement learning. In *Proceedings of the 33rd International Conference on Machine Learning*.

Mnih, V., Kavukcuoglu, K., Silver, D., Rusu, A. A., Veness, J., Bellemare, M. G., Graves, A., Riedmiller, M., Fidjeland, A. K., Ostrovski, G., et al. (2015). Human-level control through deep reinforcement learning. *Nature*.

Mousavi, A., Li, L., Liu, Q., and Zhou, D. (2020). Black-box off-policy estimation for infinite-horizon reinforcement learning. In *International Conference on Learning Representations*.

Nachum, O., Chow, Y., Dai, B., and Li, L. (2019a). Dualdice: Behavior-agnostic estimation of discounted stationary distribution corrections. *arXiv preprint arXiv:1906.04733*.

Nachum, O., Dai, B., Kostrikov, I., Chow, Y., Li, L., and Schuurmans, D. (2019b). Algaedice: Policy gradient from arbitrary experience. *arXiv preprint arXiv:1912.02074*.

OpenAI (2018). Openai five. <https://openai.com/five/>.

Osband, I., Aslanides, J., and Cassirer, A. (2018). Randomized prior functions for deep reinforcement learning. In *Advances in Neural Information Processing Systems*.

Papini, M., Binaghi, D., Canonaco, G., Pirotta, M., and Restelli, M. (2018). Stochastic variance-reduced policy gradient. *arXiv preprint arXiv:1806.05618*.

Parker, D. (2009). Managing risk in healthcare: understanding your safety culture using the manchester patient safety framework (mapsaf). *Journal of nursing management*.

Prashanth, L. and Ghavamzadeh, M. (2013). Actor-critic algorithms for risk-sensitive mdps. In *Advances in neural information processing systems*.

Precup, D., Sutton, R. S., and Dasgupta, S. (2001). Off-policy temporal-difference learning with function approximation. In *Proceedings of the 18th International Conference on Machine Learning*.

Puterman, M. L. (2014). *Markov decision processes: discrete stochastic dynamic programming*. John Wiley & Sons.

Saha, A. and Tewari, A. (2010). On the finite time convergence of cyclic coordinate descent methods. *arXiv preprint arXiv:1005.2146*.

Saha, A. and Tewari, A. (2013). On the nonasymptotic convergence of cyclic coordinate descent methods. *SIAM Journal on Optimization*, 23(1):576–601.

Schulman, J., Levine, S., Abbeel, P., Jordan, M., and Moritz, P. (2015). Trust region policy optimization. In *Proceedings of the 32nd International Conference on Machine Learning*.

Schulman, J., Wolski, F., Dhariwal, P., Radford, A., and Klimov, O. (2017). Proximal policy optimization algorithms. *arXiv preprint arXiv:1707.06347*.

Senior, A., Jumper, J., and Hassabis, D. (2018). AlphaFold: Using ai for scientific discovery. *DeepMind. Recuperado de: https://deepmind.com/blog/alphafold*.

Silver, D., Huang, A., Maddison, C. J., Guez, A., Sifre, L., Van Den Driessche, G., Schrittwieser, J., Antonoglou, I., Panneershelvam, V., Lanctot, M., et al. (2016). Mastering the game of go with deep neural networks and tree search. *Nature*.

Silver, D., Lever, G., Heess, N., Degris, T., Wierstra, D., and Riedmiller, M. (2014). Deterministic policy gradient algorithms. In *Proceedings of the 31st International Conference on Machine Learning*.

Sobel, M. J. (1982). The variance of discounted markov decision processes. *Journal of Applied Probability*.

Sutton, R. S. (1988). Learning to predict by the methods of temporal differences. *Machine Learning*.

Sutton, R. S. and Barto, A. G. (2018). *Reinforcement Learning: An Introduction (2nd Edition)*. MIT press.

Sutton, R. S., McAllester, D. A., Singh, S. P., and Mansour, Y. (2000). Policy gradient methods for reinforcement learning with function approximation. In *Advances in Neural Information Processing Systems*.

Tamar, A., Di Castro, D., and Mannor, S. (2012). Policy gradients with variance related risk criteria. *arXiv preprint arXiv:1206.6404*.

Tamar, A., Glassner, Y., and Mannor, S. (2015). Optimizing the cvar via sampling. In *Proceedings of the 29th AAAI Conference on Artificial Intelligence*.

Thomas, P. and Brunskill, E. (2016). Data-efficient off-policy policy evaluation for reinforcement learning. In *International Conference on Machine Learning*, pages 2139–2148.

Thomas, P. S., Theocharous, G., and Ghavamzadeh, M. (2015). High-confidence off-policy evaluation. In *Twenty-Ninth AAAI Conference on Artificial Intelligence*.

Tseng, P. (2001). Convergence of a block coordinate descent method for nondifferentiable minimization. *Journal of optimization theory and applications*, 109(3):475–494.

Van Seijen, H., Fatemi, M., and Tavakoli, A. (2019). Using a logarithmic mapping to enable lower discount factors in reinforcement learning. In *Advances in Neural Information Processing Systems*.

Vinyals, O., Babuschkin, I., Czarnecki, W. M., Mathieu, M., Dudzik, A., Chung, J., Choi, D. H., Powell, R., Ewalds, T., Georgiev, P., et al. (2019). Grandmaster level in starcraft ii using multi-agent reinforcement learning. *Nature*.

Wang, S. S. (2000). A class of distortion operators for pricing financial and insurance risks. *Journal of risk and insurance*.

Watkins, C. J. and Dayan, P. (1992). Q-learning. *Machine Learning*.

Williams, R. J. (1992). Simple statistical gradient-following algorithms for connectionist reinforcement learning. *Machine learning*.

Wright, S. J. (2015). Coordinate descent algorithms. *Mathematical Programming*, 151(1):3–34.

Xie, T., Liu, B., Xu, Y., Ghavamzadeh, M., Chow, Y., Lyu, D., and Yoon, D. (2018). A block coordinate ascent algorithm for mean-variance optimization. In *Advances in Neural Information Processing Systems*.

Xu, Z., van Hasselt, H. P., and Silver, D. (2018). Meta-gradient reinforcement learning. In *Advances in neural information processing systems*.

Zhang, R., Dai, B., Li, L., and Schuurmans, D. (2020a). Gendice: Generalized offline estimation of stationary values. In *International Conference on Learning Representations*.

Zhang, S., Liu, B., and Whiteson, S. (2020b). Gradientdice: Rethinking generalized offline estimation of stationary values. *arXiv preprint arXiv:2001.11113*.

## A Proofs

### A.1 Proof of Theorem 1

*Proof.*

$$\begin{aligned}
& J_\lambda(\pi_{k+1}) \\
&= \sum_{s,a} d_{\pi_{k+1}}(s,a)(r(s,a) - \lambda r(s,a)^2) + \lambda \max_y (2 \sum_{s,a} d_{\pi_{k+1}}(s,a)r(s,a)y - y^2) \\
&\geq \sum_{s,a} d_{\pi_{k+1}}(s,a)(r(s,a) - \lambda r(s,a)^2) + \lambda (2 \sum_{s,a} d_{\pi_{k+1}}(s,a)r(s,a)y_{k+1} - y_{k+1}^2) \\
&= \sum_{s,a} d_{\pi_{k+1}}(s,a)(r(s,a) - \lambda r(s,a)^2 + 2\lambda r(s,a)y_{k+1}) - \lambda y_{k+1}^2 \\
&\geq \sum_{s,a} d_{\pi_k}(s,a)(r(s,a) - \lambda r(s,a)^2 + 2\lambda r(s,a)y_{k+1}) - \lambda y_{k+1}^2
\end{aligned}$$

(By definition,  $\pi_{k+1}$  is the maximizer.)

$$\begin{aligned}
&= \sum_{s,a} d_{\pi_k}(s,a)(r(s,a) - \lambda r(s,a)^2) + \lambda (2 \sum_{s,a} d_{\pi_k}(s,a)r(s,a)y_{k+1} - y_{k+1}^2) \\
&= \sum_{s,a} d_{\pi_k}(s,a)(r(s,a) - \lambda r(s,a)^2) + \lambda \max_y (2 \sum_{s,a} d_{\pi_k}(s,a)r(s,a)y - y^2)
\end{aligned}$$

(By definition,  $y_{k+1}$  is the maximizer of the quadratic.)

$$= J_\lambda(\pi_k)$$

□

### A.2 Proof of Theorem 2

**Lemma 1.** *Under Assumption 1,  $\nabla_\theta J_\lambda(\theta)$  is Lipschitz continuous in  $\theta$ .*

*Proof.* By definition,

$$\nabla J_\lambda(\theta) = \nabla \mathbb{E}[R] - \nabla \lambda \mathbb{E}[R^2] + 2\lambda \mathbb{E}[R] \nabla \mathbb{E}[R].$$

The policy gradient theorem (Sutton et al., 2000) and the boundedness of  $\nabla \log \pi_\theta(a|s)$  imply that  $\nabla \mathbb{E}[R]$  is bounded. So  $\mathbb{E}[R]$  is Lipschitz continuous. Lemma B.2 in Papini et al. (2018) shows that the Hessian of  $\mathbb{E}[R]$  is bounded. So  $\nabla \mathbb{E}[R]$  is Lipschitz continuous. So does  $\nabla \mathbb{E}[R^2]$ . Together with the boundedness of  $\mathbb{E}[R]$ , it is easy to see  $\nabla J_\lambda(\theta)$  is Lipschitz continuous. □

We now prove Theorem 2.

*Proof.* As  $J_\lambda(\theta, y)$  is quadratic in  $y$ , the maximizing  $y$  for each  $\theta$  can be computed analytically as  $(1 - \gamma)J(\theta)$ . As rewards are bounded, we have  $\sup_{\theta \in \Theta} |J(\theta)| < \infty$ , allowing us to specify a compact set  $Y \subset \mathbb{R}$  such that for each  $\theta$ ,  $(1 - \gamma)J(\theta) \in Y$ , i.e., for each  $\theta$ ,  $\arg \max_y J_\lambda(\theta, y) = \arg \max_{y \in Y} J_\lambda(\theta, y)$ . This means our search for  $y_{k+1}$  is also conducted within a compact set. Then Theorem 4.1(c) in Tseng (2001) shows the limit of any convergent subsequence  $\{(\theta_k, y_k)\}_{k \in \mathcal{K}}$ , referred to as  $(\theta_K, y_K)$ , satisfies  $\nabla_\theta J_\lambda(\theta_K, y_K) = 0$  and  $\nabla_y J_\lambda(\theta_K, y_K) = 0$ . In particular, that Theorem 4.1(c) is developed for general block coordinate ascent algorithms with  $M$  blocks. Our MVPI is a special case with two blocks (i.e.,  $\theta$  and  $y$ ). With only two blocks, the conclusion of Theorem 4.1(c) follows immediately from Eq (7) and Eq (8) in Tseng (2001), without involving the assumption that the maximizers of the  $M - 2$  blocks are unique.

As  $J_\lambda(\theta, y)$  is quadratic in  $y$ ,  $\nabla_y J_\lambda(\theta_K, y_K) = 0$  implies  $y_K = \arg \max_y J_\lambda(\theta_K, y) = (1-\gamma)J(\theta_K)$ . Recall the Fenchel duality  $x^2 = \max_z f(x, z)$ , where  $f(x, z) \doteq 2xz - z^2$ . Applying Danskin's theorem (Proposition B.25 in Bertsekas (1995)) to Fenchel duality yields

$$\frac{\partial x^2}{\partial x} = \frac{\partial f(x, \arg \max_z f(x, z))}{\partial x}. \quad (5)$$

Note Danskin's theorem shows that we can treat  $\arg \max_z f(x, z)$  as a constant independent of  $x$  when computing the gradients in the RHS of Eq (5). Applying Danskin's theorem in the Fenchel duality used in Eq (2) yields

$$\nabla_\theta J_\lambda(\theta_K) = \nabla_\theta J_\lambda(\theta_K, y_K) = 0. \quad (6)$$

Eq (6) can also be easily verified without invoking Danskin's theorem by expanding the gradients explicitly. Eq (6) indicates that the subsequence  $\{\theta_k\}_{k \in \mathcal{K}}$  converges to a stationary point of  $J_\lambda(\theta)$ .

Theorem 1 establishes the monotonic policy improvement when we search over all possible policies (The  $\arg \max$  of Step 2 in Algorithm 1 is taken over all possible policies). Fortunately, the proof of Theorem 1 can also be used (up to a change of notation) to establish that

$$J_\lambda(\theta_{k+1}) \geq J_\lambda(\theta_k). \quad (7)$$

In other words, the monotonic policy improvement also holds when we search over  $\Theta$ . Eq (7) and the fact that  $J_\lambda(\theta)$  is bounded above imply that  $\{J_\lambda(\theta_k)\}_{k=1,\dots}$  converges to some  $J_*$ .

Let  $\Theta_* \doteq \{\theta \in \Theta | J_\lambda(\theta) = J_*\}$ . As  $\Theta$  is compact,  $J_\lambda(\theta)$  is continuous in  $\theta$ , the image of  $J_\lambda$  is then compact, indicating  $J_*$  is in the image of  $J_\lambda$ .  $\Theta_*$  is, therefore, not empty. Assumption 1 and Lemma 1 imply  $\{\theta_k\}$  converges to  $\Theta_*$ , aka,  $\lim_{t \rightarrow \infty} d(\theta_k, \Theta_*) = 0$ , where  $d(\theta_k, \Theta_*) = \inf_{\theta \in \Theta_*} \|\theta_k - \theta\|$ . It is easy to see  $\Theta_*$  is union of disjoint sets  $\{\Theta_1, \Theta_2, \dots, \Theta_N\}$ , where  $\Theta_i$  is either a plateau of  $J_\lambda(\theta)$  or a singleton. We now break  $\{\theta_k\}_{k=1,\dots}$  into several subsequences  $\{\mathcal{K}_1, \mathcal{K}_2, \dots, \mathcal{K}_N\}$  according to the distance from  $\{\Theta_1, \Theta_2, \dots, \Theta_N\}$ . Namely, we define  $\mathcal{K}_i \doteq \{k | d(\theta_k, \Theta_i) \leq d(\theta_k, \Theta_j) \forall j \neq i\}$ . (1) If  $\mathcal{K}_i$  is finite, it does not influence the asymptotic behavior of  $\{\theta_k\}$ . We, therefore, consider only infinite  $\mathcal{K}_i$ . (2) If  $\Theta_i$  is a singleton, then  $\{\theta_k\}_{k \in \mathcal{K}_i}$  is a convergent subsequence, implying  $\{\theta_k\}_{k \in \mathcal{K}_i}$  converges to a stationary point, i.e.,  $\{\|\nabla_\theta J_\lambda(\theta_k)\|\}_{k \in \mathcal{K}_i}$  converges to 0. (3) If  $\Theta_i$  is a plateau,  $\|\nabla_\theta J_\lambda(\theta)\| = 0$  holds for all  $\theta \in \Theta_i$ . As  $\{\theta_k\}_{k \in \mathcal{K}_i}$  converges to  $\Theta_i$  and  $\nabla_\theta J_\lambda(\theta)$  is Lipschitz continuous in  $\theta$ , we have  $\{\|\nabla_\theta J_\lambda(\theta_k)\|\}_{k \in \mathcal{K}_i}$  converges to 0. Putting (1), (2), and (3) together, we have  $\lim_{t \rightarrow \infty} \|\nabla_\theta J_\lambda(\theta_k)\| = 0$ . Note this does not imply that  $\{\theta_k\}$  converges, it is possible that  $\{\theta_k\}$  wanders among different stationary points. This is due to the nature of BCCA as the maximization in BCCA is a global operation.  $\square$

## B Experiment Details

The pseudocode of MVPI-TD3 and our TRVO (MVPI-PPO) are provide in Algorithms 3 and 4 respectively.

**Task Selection:** We use eight Mujoco tasks from Open AI gym <sup>4</sup>(Brockman et al., 2016) and implement the tabular MDP in Figure 2a by ourselves.

**Function Parameterization:** For MVPI-TD3 and TD3, we use the same network architecture as Fujimoto et al. (2018). For TRVO (MVPI-PPO), the methods of Tamar et al. (2012); Prashanth and Ghavamzadeh (2013), and MVP, we use the same network architecture as Schulman et al. (2017).

**Hyperparameter Tuning:** For MVPI-TD3 and TD3, we use the same hyperparameters as Fujimoto et al. (2018). In particular, for MVPI-TD3, we set  $K = 10^4$ . For TRVO (MVPI-PPO), we use the same hyperparameters as Schulman et al. (2017). We implement the methods of Prashanth and Ghavamzadeh (2013); Tamar et al. (2012) and MVP with multiple parallelized actors like A2C in Dhariwal et al. (2017) and inherit the common hyperparameters from Dhariwal et al. (2017).

**Hyperparameters of Prashanth and Ghavamzadeh (2013):** To increase stability, we treat  $\lambda$  as a hyperparameter instead of a variable. Consequently,  $\xi$  does not matter. We tune  $\lambda$  from  $\{0.5, 1, 2\}$ . We set the perturbation  $\beta$  in Prashanth and Ghavamzadeh (2013) to  $10^{-4}$ . We use 16 parallelized actors. The initial learning rate of the RMSprop optimizer is  $7 \times 10^{-5}$ , tuned from  $\{7 \times 10^{-5}, 7 \times 10^{-6}\}$ .

<sup>4</sup><https://gym.openai.com/>

---

**Algorithm 3:** MVPI-TD3

---

**Input:**

$\theta, \psi$ : parameters for the deterministic policy  $\pi$  and the value function  $q_\pi$   
 $K$ : number of recent rewards for estimating the policy performance  
 $\lambda$ : weight of the variance penalty

```
Initialize the replay buffer  $\mathcal{M}$ 
Initialize  $S_0$ 
for  $t = 0, \dots, \text{do}$ 
   $A_t \leftarrow \pi(S_t) + \mathcal{N}(0, \sigma^2)$ 
  Execute  $A_t$ , get  $R_{t+1}, S_{t+1}$ 
  Store  $(S_t, A_t, R_{t+1}, S_{t+1})$  into  $\mathcal{M}$ 
   $y \leftarrow \frac{1}{K} \sum_{i=t-K+2}^{t+1} R_t$ 
  Sample a mini-batch  $\{s_i, a_i, r_i, s'_i\}_{i=1, \dots, N}$  from  $\mathcal{M}$ 
  for  $i = 1, \dots, N$  do
     $\hat{r}_i \leftarrow r_i - \lambda r_i^2 + 2\lambda r_i y$ 
  end
  Use TD3 with  $\{s_i, a_i, \hat{r}_i, s'_i\}_{i=1, \dots, N}$  to optimize  $\theta$  and  $\psi$ 
   $t \leftarrow t + 1$ 
end
```

---

---

**Algorithm 4:** MVPI-PPO

---

**Input:**

$\theta, \psi$ : parameters for the policy  $\pi$  and the value function  $v_\pi$   
 $K, \lambda$ : rollout length and weight for variance

```
while True do
  Empty a buffer  $\mathcal{M}$ 
  Run  $\pi$  for  $K$  steps in the environment, storing  $\{s_i, a_i, r_i, s_{i+1}\}_{i=1, \dots, K}$  into  $\mathcal{M}$ 
   $y \leftarrow \frac{1}{K} \sum_{i=1}^K r_i$ 
  for  $i = 1, \dots, K$  do
     $\hat{r}_i \leftarrow r_i - \lambda r_i^2 + 2\lambda r_i y$ 
  end
  Use PPO with  $\{s_i, a_i, \hat{r}_i, s_{i+1}\}_{i=1, \dots, K}$  to optimize  $\theta$  and  $\psi$ 
end
```

---

$10^{-4}, 7 \times 10^{-3}\}$ . We also test the Adam optimizer, which performs the same as the RMSprop optimizer. We use policy entropy as a regularization term, whose weight is 0.01. The discount factor is 0.99. We clip the gradient by norm with a threshold 0.5.

**Hyperparameters of Tamar et al. (2012):** We tune  $\lambda$  from  $\{0.5, 1, 2\}$ . We use  $\xi = 50$ , tuned from  $\{1, 10, 50, 100\}$ . We set the initial learning rate of the RMSprop optimizer to  $7 \times 10^{-4}$ , tuned from  $\{7 \times 10^{-5}, 7 \times 10^{-4}, 7 \times 10^{-3}\}$ . We also test the Adam optimizer, which performs the same as the RMSprop optimizer. The learning rates for the running estimates of  $\mathbb{E}[G_0]$  and  $\mathbb{V}(G_0)$  is 100 times of the initial learning rate of the RMSprop optimizer. We use 16 parallelized actors. We use policy entropy as a regularization term, whose weight is 0.01. We clip the gradient by norm with a threshold 0.5.

**Hyperparameters of Xie et al. (2018):** We tune  $\lambda$  from  $\{0.5, 1, 2\}$ . We set the initial learning rate of the RMSprop optimizer to  $7 \times 10^{-4}$ , tuned from  $\{7 \times 10^{-5}, 7 \times 10^{-4}, 7 \times 10^{-3}\}$ . We also test the Adam optimizer, which performs the same as the RMSprop optimizer. We use 16 parallelized actors. We use policy entropy as a regularization term, whose weight is 0.01. We clip the gradient by norm with a threshold 0.5.

**Computing Infrastructure:** We conduct our experiments on an Nvidia DGX-1 with PyTorch, though no GPU is used.

In our off-line off-policy experiments, we set  $K$  to  $10^3$  and use tabular representation for  $\rho_\pi, q_\pi$ . For  $\pi$ , we use a softmax policy with tabular logits.

## C Other Experimental Results

We report the empirical results with  $\lambda = 0.5$  and  $\lambda = 2$  in Figure 3, Table 2, Figure 4, and Table 3.

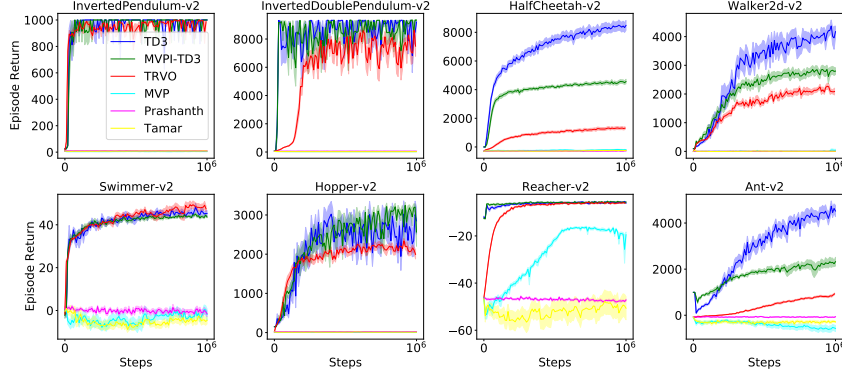


Figure 3: Figure 1 with  $\lambda = 0.5$ .

	$\Delta_J^{\text{TRVO}}$	$\Delta_{\text{mean}}^{\text{TRVO}}$	$\Delta_{\text{variance}}^{\text{TRVO}}$	$\Delta_J^{\text{MVPI-TD3}}$	$\Delta_{\text{mean}}^{\text{MVPI-TD3}}$	$\Delta_{\text{variance}}^{\text{MVPI-TD3}}$
InvertedPendulum	-581%	-3%	$10^8\%$	0%	0%	-100%
InvertedDoublePendulum	-1407%	-24%	1337%	-10%	0%	10%
HalfCheetah	83%	-84%	-83%	66%	-46%	-65%
Walker2d	-44%	-51%	42%	91%	-34%	-90%
Swimmer	0%	4%	264%	-4%	-4%	4%
Hopper	-19%	-28%	18%	74%	-10%	-73%
Reacher	-26%	-4%	80%	3%	5%	2%
Ant	93%	-81%	-92%	88%	-49%	-88%

Table 2: Table 1 with  $\lambda = 0.5$ .

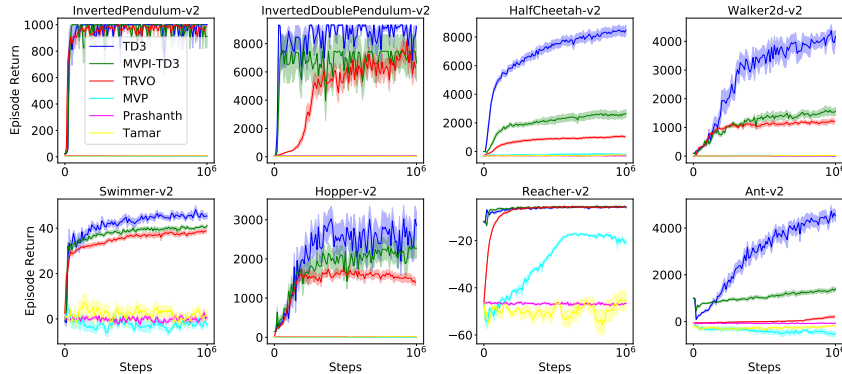


Figure 4: Figure 1 with  $\lambda = 2$ .

	$\Delta_j^{\text{TRVO}}$	$\Delta_{\text{mean}}^{\text{TRVO}}$	$\Delta_{\text{variance}}^{\text{TRVO}}$	$\Delta_j^{\text{MVPI-TD3}}$	$\Delta_{\text{mean}}^{\text{MVPI-TD3}}$	$\Delta_{\text{variance}}^{\text{MVPI-TD3}}$
InvertedPendulum	-1719%	-2%	10 <sup>8</sup> %	-9%	-9%	16309%
InvertedDoublePendulum	-1707%	-31%	1686%	78%	-28%	-77%
HalfCheetah	92%	-88%	-92%	96%	-69%	-96%
Walker2d	78%	-71%	-78%	98%	-63%	-98%
Swimmer	-80%	-15%	1151%	-24%	-11%	231%
Hopper	73%	-49%	-73%	78%	-20%	-77%
Reacher	-34%	1%	55%	4%	3%	-5%
Ant	97%	-95%	-97%	99%	-69%	-99%

Table 3: Table 1 with  $\lambda = 2$ .